Prabha Materials Science Letters
Vol. 3, No. 1, 1-28, 2024
https://doi.org/10.33889/PMSL.2024.3.1.001

Ram Arti Publishers

Physical Property Variation of Ferrite Nanoparticles under Heavy Ion Irradiation

Reena Dhyani
Department of Applied Science,
Women Institute of Technology, Dehradun, 248007, Uttarakhand, India.
E-mail: reenadhyani16@gmail.com

Amit Joshi
Department of Physics,
Govind Ballabh Pant University of Agriculture & Technology, Pantnagar, 263145, Uttarakhand, India.
E-mail: amit.phy.1216@gmail.com

Vimal Narayan Sahoo
Department of Physics, School of Physical,
Chemical and Applied Sciences, Pondicherry University, Kalapet, 605014, Puducherry, India.
E-mail: vimalsahoo1997@pondiuni.ac.in

Jitendra Pal Singh
Department of Sciences (Physics),
Manav Rachna University, Faridabad,121004, Haryana, India.
Corresponding author: jpsingh@mru.edu.in

(Received on January 14, 2023; Revised on August 11, 2023; Accepted on September 19, 2023)

Abstract
The size-dependent behavior of nanostructured ferrite is well established. Various physical properties such as magnetic, optical and electrical exhibit strong size dependence. Thus, any treatment which causes a change in size is able to modify the characteristics of ferrites. The result of this effect can be seen when these ferrites are subjected to an intense heavy ion beam which modifies the physical properties of ferrites. This modification is related to cation redistribution owing to size change in most of the cases under heavy ion irradiation. However, few recent studies show that cation redistribution may occur under ion irradiation even though no size change is observed. The objective of this review is to highlight this effect in ferrite systems which ultimately may provide ample opportunity for its potential applications.

Keywords- Ion irradiation, Ferrites, Cation occupancy, Size independence.

1. Introduction

Ferrites have been a well-known system to mankind for a long time (Lord & Parker, 1960; Grimes, & Collett, 1971; Sato et al., 1987). These ferrites have the formula MFe_2O_4, where, M is a transition metal (TM) ion and exhibits ferrimagnetic character in the bulk form (Brockman, 1951). One can alter the magnetic behavior of these ferrites by replacing M with appropriate transition metals (Smit & Wijn, 1954). Thus, the selection of TM ions is required while designing these ferrites for specific applications when they are used in bulk form. This leads to the growth of zinc ferrite, manganese ferrite, cobalt ferrite, nickel ferrite, nickel-zinc ferrite etc. (Table 1). Changes in microstructure or external treatment are also responsible for modification in the physical behavior of ferrites by altering cation inversion (Zhuravlev et al., 1990; Singh et al., 2013; Peng et al., 2017). Cation inversion is a frequently used term in ferrite and details can be found in many reports (Torruella et al., 2018; Nandy et al., 2022).

Table 1. Design of various ferrites while replacing M^{2+} in MFe_2O_4 with suitable TM ions.

M^{2+}	Magnetic Nature in Bulk Form at room temperature	Application
Zn^{2+}	Paramagnetic	Gas desulpherisation (Jha et al., 1988; Cilleruelo et al., 1995)
Ni^{2+}	Ferrimagnetic	Magnetic shielding (Narang et al., 2021)
Co^{2+}	Ferrimagnetic, Highly Coercive	Permanent Magnets (Lamouri et al., 2020a)
Mn^{2+}	Ferrimagnetic	Soft Magnetic applications (Aslibeiki et al., 2016)

These materials are still being explored because of the induction of numerous phenomena and applications that arise because of nano dimensions (Mohapatra et al., 2019; Singh et al., 2023a; Hublikar et al., 2023). The main characteristic of ferrite nanostructures is the size dependence of their physical properties when synthesized in nanoregime. Especially, these ferrite nanostructures are known for their altered magnetic behavior compared to their bulk counterpart (Liu and Zhang, 2001; Fantauzzi et al., 2019). Paramagnetic zinc ferrite (Singh et al., 2008) may transform to superparamagnetic (Singh et al., 2008; Hasirci et al., 2019), ferromagnetic (Li et al., 2011) and ferromagnetic (Raghavan et al., 2015) at room temperature depending upon size. Reports are available showing soft magnetic properties of $CoFe_2O_4$ when size is reduced to nano dimension (Zorai et al., 2023). Figure 1 depicts the magnetic behavior of ferrite nanoparticles and thin films which shows strong size dependence. Kamble et al. (2015) observed that the room temperature magnetic nature of nickel ferrite nanoparticles of size 14 nm (NF03), 15 nm (NF04), 18 nm (NF05) and 22 nm (NF06) remain the same. All nanoparticles exhibit a ferromagnetic kind of magnetic ordering but their saturation magnetization increases from 25 to 45 emu/g as the particle size increases from 14 to 22 nm (Figure 1(a)). Copper ferrite (Kumar et al., 2019), magnesium ferrite (Šepelák et al., 2007) and cobalt ferrite (Lamouri et al., 2020) also exhibit the same behavior. Change in corecievity (H_c) with crystallite size is also reported for ferrite nanoparticles (Lu et al., 2014). Parameters such as retentivity (M_r), and anisotropy (K) are also influenced by the crystallite size (Peddis et al., 2012; Das et al., 2020). In the case of thin films too, size-dependent behavior of saturation magnetization (M_s) is reported as shown in Figure 1(b) (Dixit et al., 2012a).

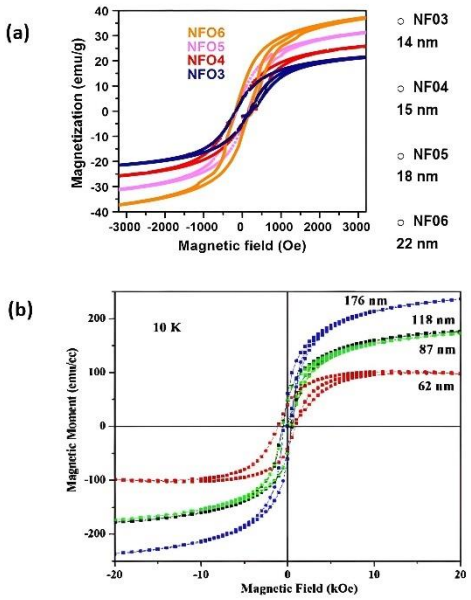

Figure 1. Magnetic Hysteresis curves of (a) nickel ferrite nanoparticles. Permission was obtained from Kamble et al. (2015) (Open access) and (b) nickel ferrite thin films. Reprinted with permission from Dixit et al. (2012a) (Open access).

Other characteristics of ferrite nanoparticles/thin films such as blocking temperature, T_B (Singh et al., 2012a; Singh et al., 2017) and Curie temperature, T_N (Sadeh et al., 2000; Fesharaki et al., 2016) also exhibit strong size dependence. Figure 2 summarizes the size dependence of various magnetic parameters for $MnFe_2O_4$ nanoparticles (Islam et al., 2020). All magnetic parameters exhibit a linear relation with the size of these nanoparticles. This figure also depicts that Yafet-Kittel (Y-K)canting angle and squareness (M_r/Msat) is influenced by the size of nanoparticles.

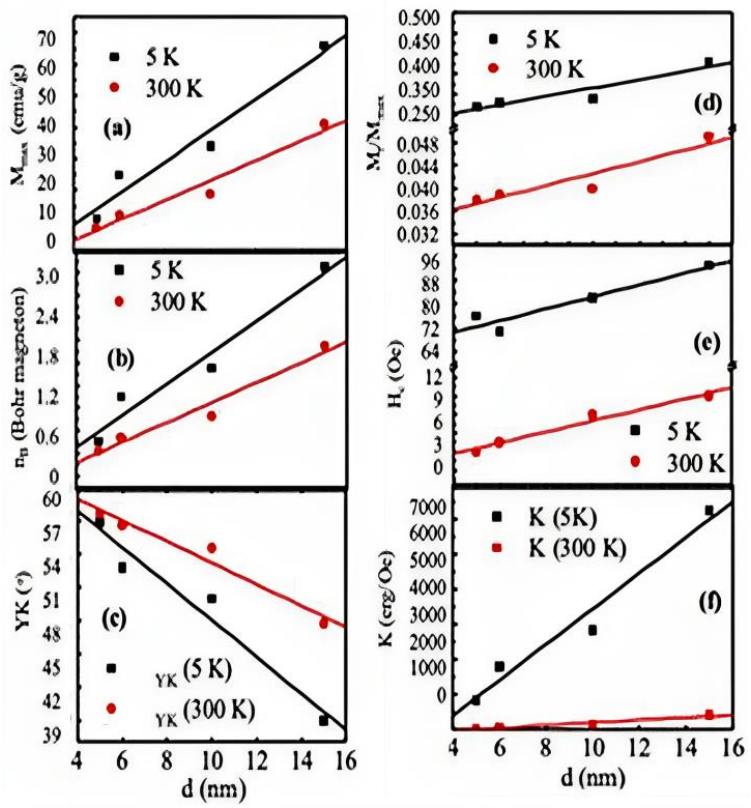

Figure 2. (a) Maximum magnetization (b) Bohr magneton, (c) Canting angles, (d) Squareness ratio, (e) Coercivity, and (f) Anisotropy with size variations of $MnFe_2O_4$ nanoparticles. Reprinted with permission from Islam et al. (2020).

In the same way, the optical behavior of ferrites is also affected by the crystallite size (Singh et al., 2010c; Jogi et al., 2022; Refat et al., 2022). Various ferrite nanoparticle exhibits absorbance which depends on the size of the ferrite nanoparticle. This causes a change in optical band-gap of ferrite material. An enhancement in the optical band-gap is reported for $Ni_2Fe_2O_4$ nanoparticles (Karmakar & Behera, 2020). $CoFe_2O_4$ nanoparticles also exhibit variations of optical band gap with crystallite size (Singh et al., 2020). Figure 3(a) shows the reduction in optical band-gap value with an increase of crystallite size. Similar behavior of optical band-gap is also reported by Massoudi et al. (2020) for $Ni_{0.6}Zn_{0.4}Al_{0.5}Fe_{1.5}O_4$ nanoparticles (Figure 3(b)). In the case of ferrite thin film, this parameter exhibits a strong dependence on film thickness. Figure 3(c) shows an inverse correlation between the optical band-gap and film thickness for $Ti_{0.5}Li_{0.5}La_{0.1}Fe_{1.9}O_4$ thin films (Abdelmoneim, 2010).

Figure 4(a) shows the ac conductivity behavior for cobalt ferrite nanoparticles of different sizes. This clearly shows the effect of particle size on the electrical behavior of ferrites (Yadav et al., 2017). DC conductivity of ferrite nanoparticles is influenced by the size of ferrite particles (Lahouli et al., 2019) as depicted in Figure 4(b) by the variation of conductivity with temperature.

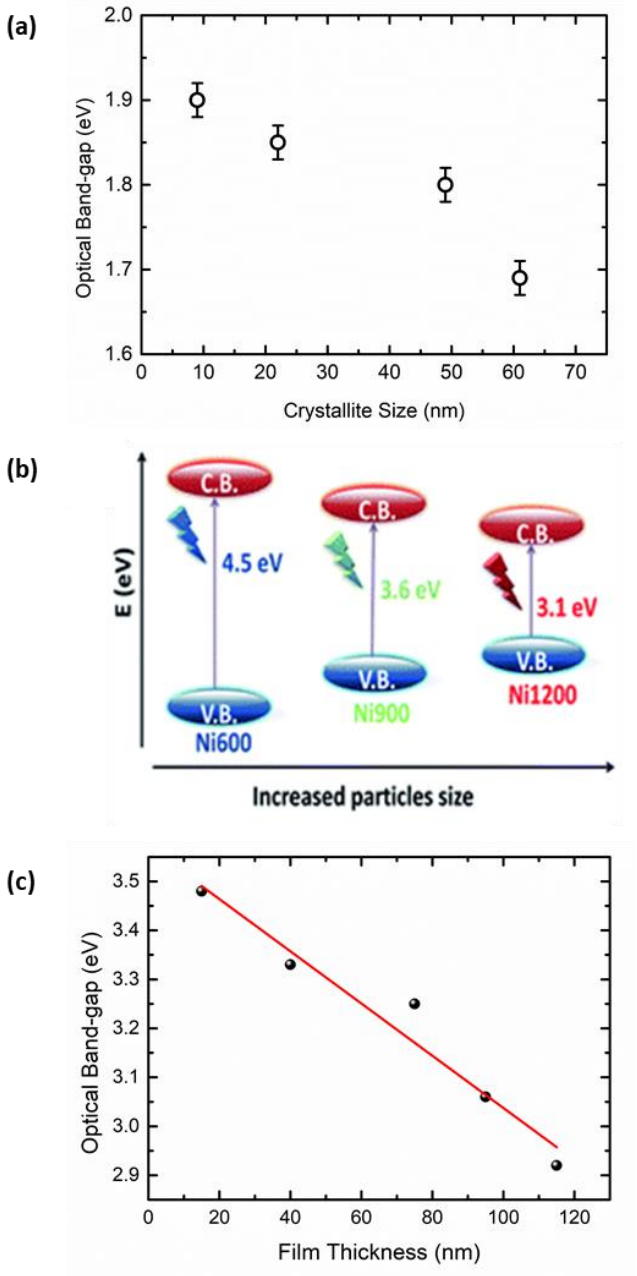

Figure 3. (a) Optical Band-gap for $CoFe_2O_4$ nanoparticles as a function of crystallite size. Permission obtained from RSC Advances (Singh et al., 2020) (b) Schematic representation of band structure at various particle sizes for $Ni_{0.6}Zn_{0.4}Al_{0.5}Fe_{1.5}O_4$ material. Preprinted with permission from Massoudi et al. (2020), Variation of optical band-gap with thickness for $Ti_{0.5}Li_{0.5}La_{0.1}Fe_{1.9}O_4$ thin films. Values of thickness and optical band gap are taken from Abdelmoneim (2010).

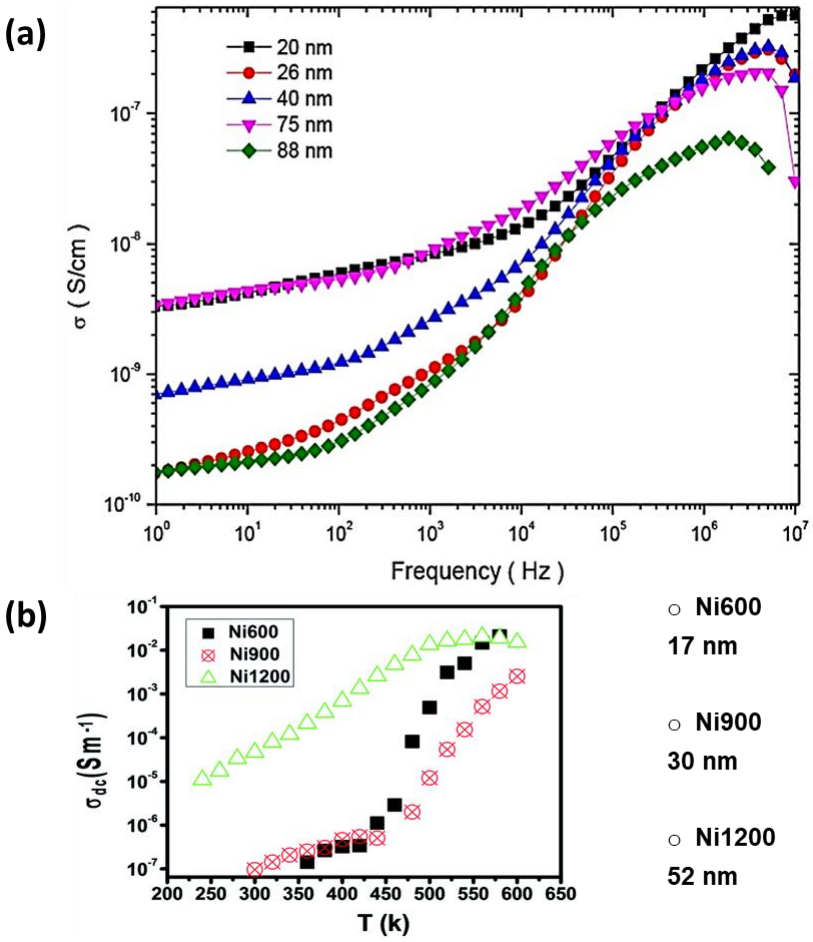

Figure 4. (a) Frequency dependent ac conductivity of cobalt ferrite nanoparticles of different sizes. Reprinted from Yadav et al. (2017) Adv. Nat. Sci: Nanosci. Nanotechnol. 8 045002 (Open access). The plot of DC conductivity versus temperature for $Ni_{0.6}Zn_{0.4}Fe_{1.5}Al_{0.5}O_4$ annealed at different temperatures. Reprinted with permission from Lahouli et al. (2019).

Not only the electrical behavior but dielectric behavior of ferrites is also affected by the size of ferrite nanoparticles. The dielectric behavior of $CoFe_2O_4$ nanoparticles of size 6 and 50 nm is depicted in Figure 5. This shows the increasing trend of dielectric permittivity with the decrease in crystallite size for $CoFe_2O_4$ nanoparticles (Vasundhara et al., 2013).

Thus, these examples show that size-dependent changes in physical properties are characteristics of ferrite nanoparticles. Depending upon the size, the physical behavior of ferrite having the same composition may differ (Mozaffari and Masoudi, 2014; Parmar et al., 2022a). The origin of size-dependent physical properties of ferrites is the result of a change in cation inversion in nanoregime (Siddique and Butt, 2010; Pham et al., 2023). A simple representation of various physical properties, their applications, size and cation distribution is shown in Figure 6 by taking the example of $CoFe_2O_4$ (Jauhar et al., 2016; Varma et al., 2016). Not only their physical behavior but their utility for particular applications is influenced by the size of ferrite nanoparticles (Noreen et al., 2017; Li et al., 2019).

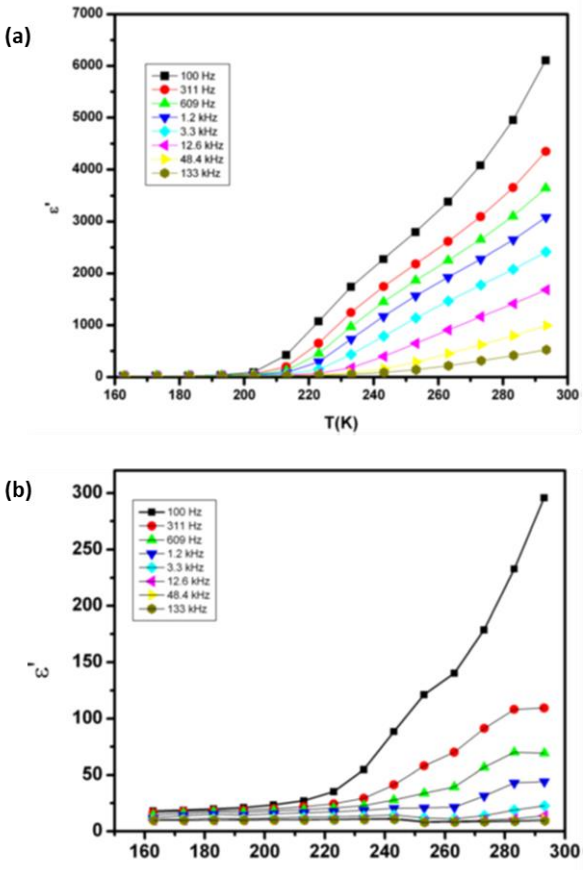

Figure 5. Variation of real part of relative permittivity with temperature in $CoFe_2O_4$ samples ((a) 6 nm sample and (b) 50 nm sample). Reprinted with permission from Vasundhara et al. (2013).

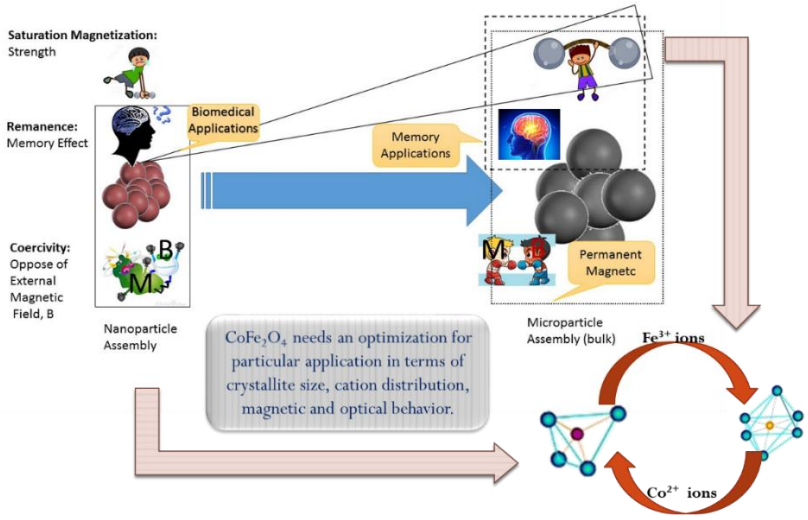

Figure 6. Schematic depicting the size dependent variation in magnetic parameters along with their applications and its correlation with cation distribution (Drawn based on the properties of $CoFe_2O_4$).

Apart from size dependence, doping of various elements is also able to change in physical properties of ferrites (Dixit et al., 2012b). Doping of particular ions too influences the crystallite and cation inversion. Thus, cation inversion is responsible for the changes in the properties of ferrites. There are certain methods such as laser irradiation (Tawfik et al., 2002; Ateia et al., 2019), ion implantation (Sharma et al., 2023a), gamma-irradiation (Raut et al., 2018) and heavy ion irradiation (Nongjai et al., 2023) which are well known to change the physical behavior of ferrites in a controlled way. This review focuses on the cation inversion manipulation and associated changes with swift heavy ion irradiation.

2. Swift Heavy Ions

Swift heavy ions (SHI) are well known to modify characteristics of the materials (Kuzmann et al., 2023; Wu et al., 2023) and devices such as spintronics (Singh et al., 2016; Zhao et al., 2019), electronic (Bharathi et al., 2016; Kumar et al., 2023) and sensing (Ramola et al., 2022). These ions have the potential to design ferrites for spintronic (Garg et al., 2023) and gas sensing applications (Bagwan et al., 2022). The basic characteristics of these ions and their production procedure can be found elsewhere (Kumar et al., 2022). These ions when penetrates through the materials lose energy into the medium. The energy loss per unit length in the medium is known as stopping power (S) which is estimated from the stopping and range of ions in matter (SRIM) code (Ziegler et al., 1985). This code also gives information of the projected range in the medium. This calculation shows that energy loss in the medium is determined by the composition of the material. Energy loss or stopping power in the medium is further divided into two categories- (1) electronic stopping, S_e and (2) nuclear stopping, S_n.

2.1 Choice of Ions and their Energy

Figure 7 shows the electronic stopping power and projected range of 100 MeV O^{7+}, 200 MeV Ag^{15+} and 150 MeV Si^{7+} for various ferrite materials (Ziegler et al., 2010). The projected range for O^{7+} is almost 4 times that of Ag^{15+}, however, it is almost twice compared to that Si^{7+} ions. This means a larger thickness material may be used to observe irradiation effects in the case of O^{7+} ion beams. On other hand, the electronic stopping power value is less compared to that of other ions. This indicates that it will cause less damage compared to other ions. To get an understanding of the damage process in these systems, the ratio of electronic stopping to nuclear stopping was determined (Ziegler et al., 2010). These values for 100 MeV O^{7+}; 200 MeV Ag^{15+} and 150 MeV Si^{8+} are collated in Table 2.

At first glance, these calculations show that the ion beam induced effects depend on the composition of ferrites and are supported by most of the studies carried on ferrites from 70's to early 90's (Pascard and Studer, 1997). In all cases, it is clear that S_e/Sn ratio is almost 10^3 (Table 1) , hence, the inelastic collision of ions with target nuclei is the dominant mechanism (Péter, 1977; Chandramohan et al., 2007), if the irradiation is carried out by these ions of energy mention in the table caption. This shows that the order of S_e is greater than S_n which is the reason for the dominance of electronic energy loss over nuclear ones for all swift heavy ions in different ferrite samples (Weber et al., 2015).

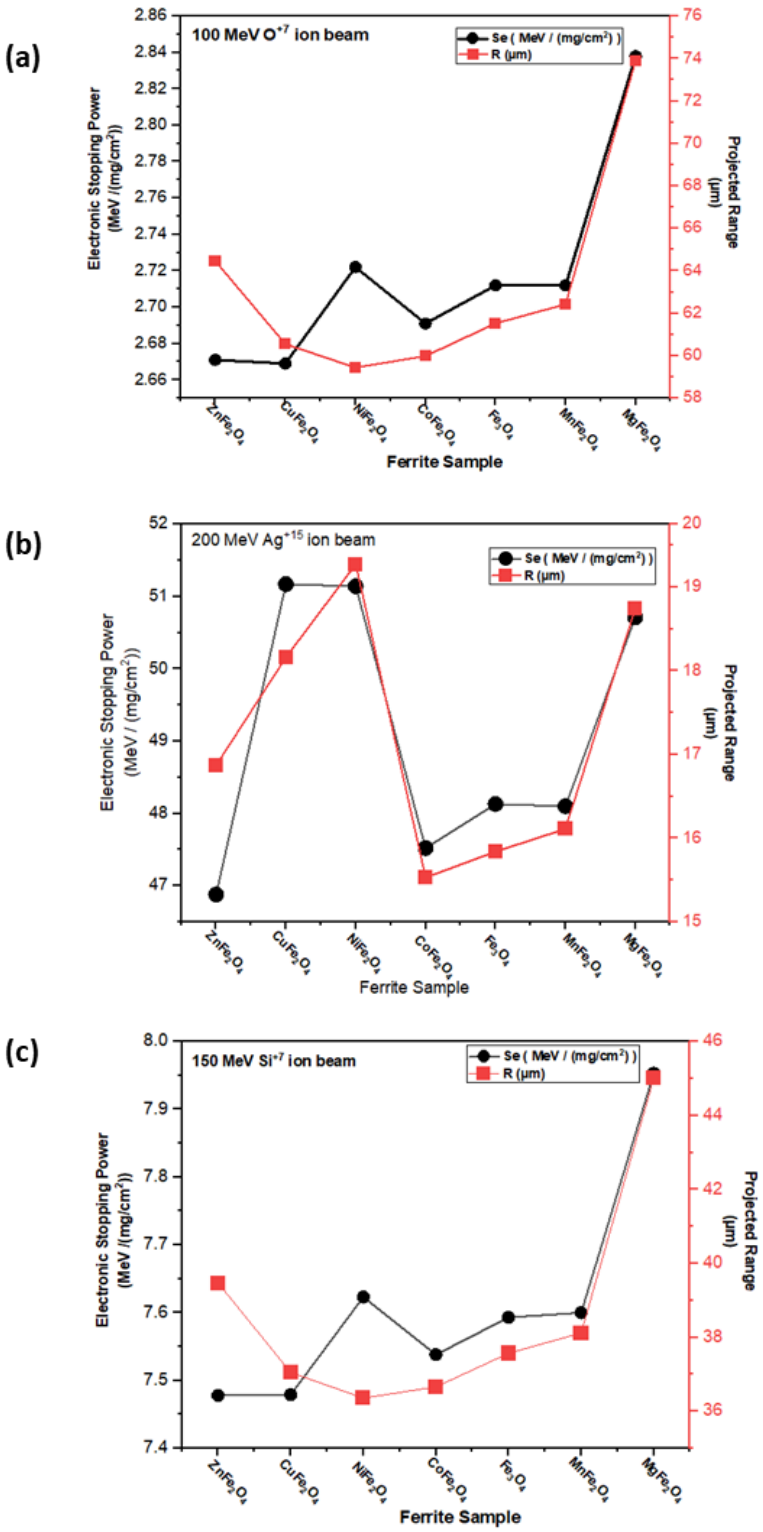

Figure 7. Electronic stopping power and projected range of various ferrites for (a) 100 MeV O^{7+} and (b) 200 MeV Ag^{15+} and (c) 150 MeV Si^{7+} ions. Values are estimated from SRIM code (Ziegler et al., 1985).

Table 2. Stopping power (S) and projected range (R) for various ions in ferrites. (Values are obtained from SRIM calculations).

Ferrite	Se (MeV / (mg/cm^2))	Sn (MeV / (mg/cm^2)	S_e/S_n Ratio (10^3)	Nature of defects
100 MeV O^{7+}				
$ZnFe_2O_4$	2.67	1.55×10^{-03}	1.76	Point defects
$CuFe_2O_4$	2.67	1.51×10^{-03}	1.76	
$NiFe_2O_4$	2.72	1.55×10^{-03}	1.76	
$CoFe_2O_4$	2.69	1.52×10^{-03}	1.77	
Fe_3O_4	2.71	1.54×10^{-03}	1.77	
$MnFe_2O_4$	2.71	1.52×10^{-03}	1.78	
$MgFe_2O_4$	2.84	1.59×10^{-03}	1.78	
200 MeV Ag^{15+}				
$ZnFe_2O_4$	46.90	1.28×10^{-01}	0.37	Columnar Defects
$CuFe_2O_4$	51.17	1.33×10^{-01}	0.39	
$NiFe_2O_4$	51.14	1.33×10^{-01}	0.38	
$CoFe_2O_4$	47.52	1.28×10^{-01}	0.37	
Fe_3O_4	48.13	1.29×10^{-01}	0.37	
$MnFe_2O_4$	48.10	1.28×10^{-01}	0.37	
$MgFe_2O_4$	50.71	1.33×10^{-01}	0.38	
150 MeV Si^{7+}				
$ZnFe_2O_4$	7.48	5.14×10^{-03}	1.45	Point/cluster defects
$CuFe_2O_4$	7.48	5.13×10^{-03}	1.46	
$NiFe_2O_4$	7.62	5.26×10^{-03}	1.45	
$CoFe_2O_4$	7.54	5.16×10^{-03}	1.46	
Fe_3O_4	7.59	5.21×10^{-03}	1.46	
$MnFe_2O_4$	7.60	5.17×10^{-03}	1.47	
$MgFe_2O_4$	7.95	5.38×10^{-03}	1.48	

Additionally, the S_e value gives information on the nature of defects formed in the system during irradiation. If Se is less than the threshold value, then point defects are created in the system, however, if it is larger than this value, then columnar defects are produced in the system. In the case of $S_e \sim S_{eth}$, both point/columnar defects are observed in the system. In the case of ferrite, the threshold value is almost 13 keV/nm as mentioned in previous work (Kumar et al., 2005). Hence, oxygen ions are known to produce point defects in ferrite materials (Singh et al., 2013). However, modifications are governed by the production of latent tracks/columnar defects in the case of Ag ions (Singh et al., 2014). In the case of Si ions, point/cluster defects are expected to induce effects in the system.

2.2 Sample Choice

In case of heavy ion irradiation, another criteria is related with the thickness of the target materials, which should always be less than the projected range. Generally, films are ideal choices for heavy ion irradiation studies as they have thickness ranging from few nm to several hundred nm, which is always less than the projected range (Panda et al., 2021; Vershney et al., 2023). Though ions penetrate through the samples, however, they reside in the substrate attached to the film (Figure 8(a)). Hence, proper care should be taken while studying the magnetic behavior of these samples.

Sometimes pellets of thickness 2-3 nm / single crystals are used for irradiation experiments (Sharma et al., 2023b; Aithal, 1997), however, post-irradiated pellets are a mixture of irradiated and unirradiated counterparts. Thus, information specific to the irradiation phenomena on the bulk physical properties is hard to obtain. In this case, only surface-related phenomena can be investigated (Figure 8(b)). To investigate, bulk behavior, very high energy of ion beam will be required in this case (Studer et al., 1993).

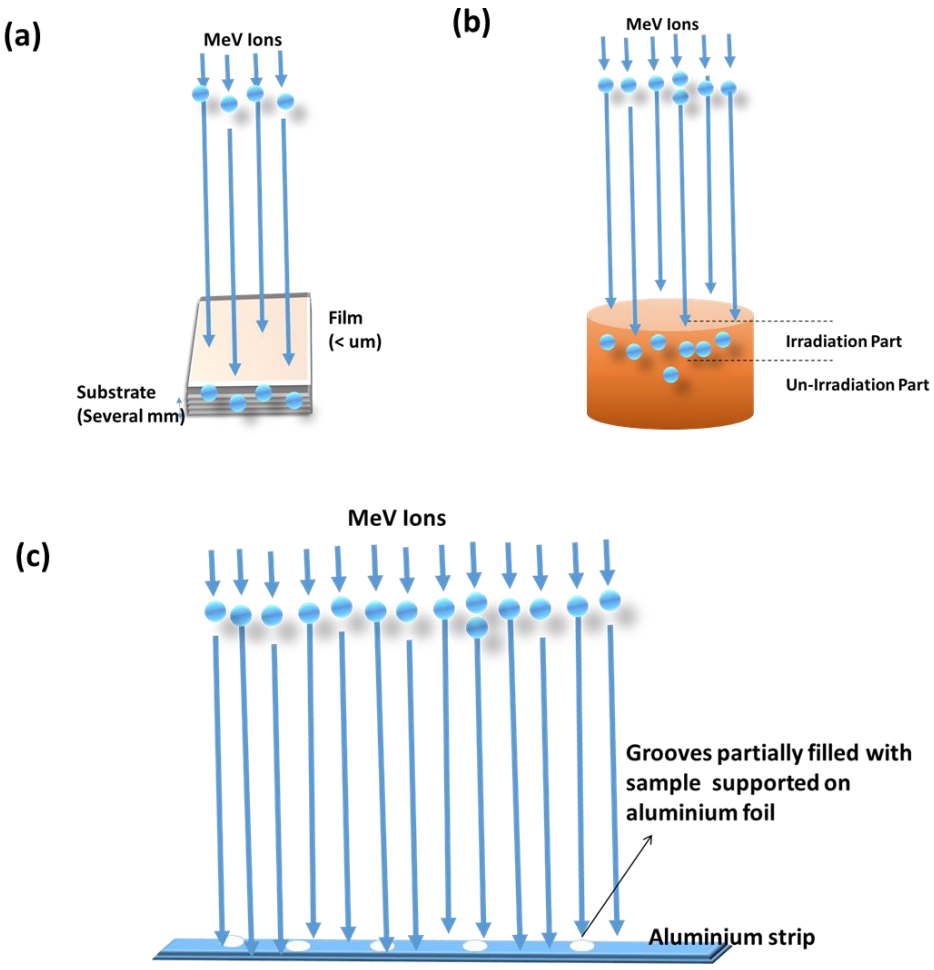

Figure 8. Irradiation procedure for (a) thin films, (b) pellets and (c) nanoparticles/powder samples.

In the case of powder materials, irradiation experiments are tricky and samples are prepared by mixing with polyvinyl alcohol (PVA) in grooves of a specific size (Srivastava et al., 2010). In these grooves, materials have volume less than the area of the groove multiplied by the projected area. Samples after irradiation are carefully taken out from the grooves and heated at 100^{o}C for removal of PVA (Figure 8(c)).

4. Experimental Results for Swift Heavy Ion Irradiation Induced Effects

4.1 Structural Properties

Heavy ions are known to induce crystallization in few systems such as ZrC films (Jiang et al., 2021), MAX nanostructures (Cannavò et al., 2021), however, most of the materials exhibit crystalline disorder after irradiation (Sathyavathi et al., 1999; Ai et al., 2019; Pang et al., 2021). Ferrites are known to be stable materials, hence, their crystalline phase remains unchanged under heavy ion irradiation as reported in most of the work. However, they too exhibit a reduced degree of crystallisation under the effect of the intense ion beam. This is evident from the X-ray diffraction studies of ferrites under heavy ion irradiation (Dixit et al., 2012c; Dolia et., 2012; Satalkar et al., 2016; Raghuvanshi et al., 2019). This motivated a number of researchers to work in this direction and the effect of swift heavy ion irradiation on the structural properties of spinel ferrite nanoparticles was investigated by various researchers. Kumar et al. observed an increase in

crystalline disorder on irradiating $CoFe_{1.90}Dy_{0.10}O_4$ nanoparticles with 100 MeV O^{7+} ions at varying fluences. It was inferred that with higher fluence more energy was deposited inside the material which resulted in deterioration of crystalline structure. Figure 9(a) shows XRD patterns of Dy doped $CoFe_2O_4$ nanoparticles. These patterns exhibit that the crystalline phase remains unchanged under irradiation of 100 MeV O^{7+} ions (Kumar et al., 2015a). However, onsets of decreased crystalline order are observed from the decreased intensity of XRD peaks. Similar behavior of XRD patterns is observed for zinc ferrite nanoparticles under the same ion beam (Figure 9(b)).

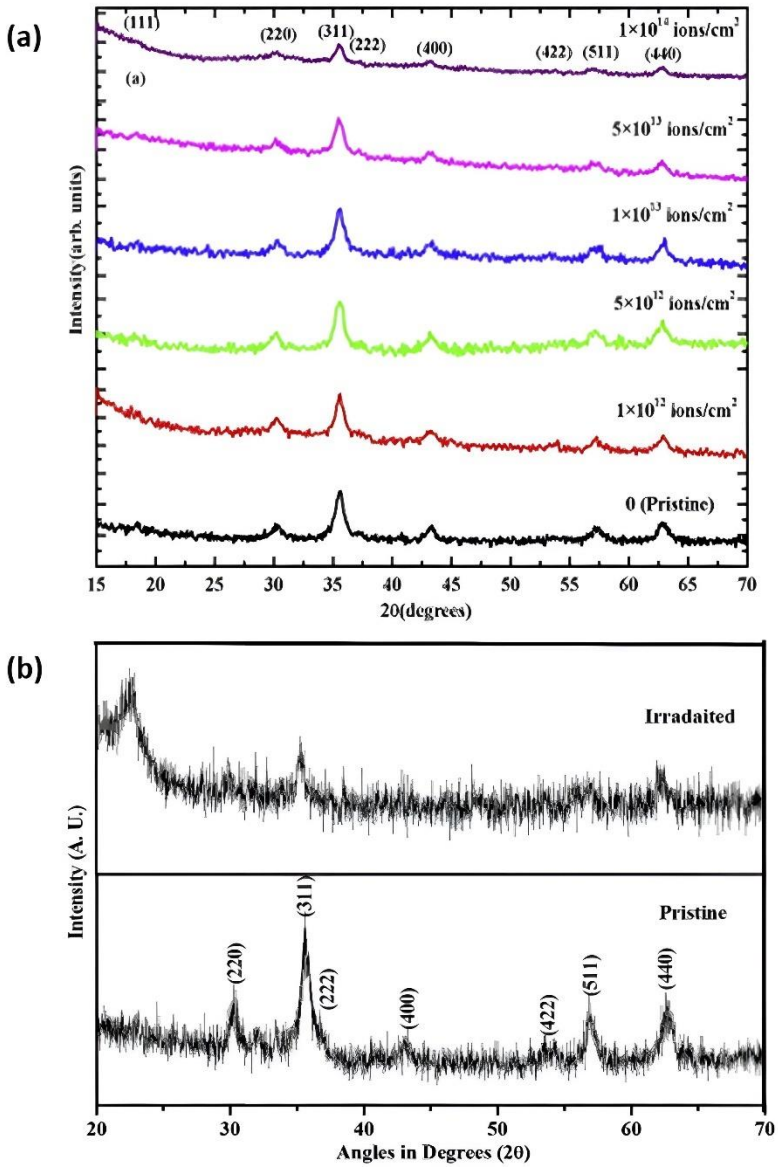

Figure 9. (a) XRD patterns of Dy deoped $CoFe_2O_4$ nanoparticles under irradiation of 100 MeV O^{7+} Reprinted with permission from Kumar et al. (2015a), (b) XRD patterns of pristine and irradiated $ZnFe_2O_4$ (5×10^{13} ions/cm^2) reprinted with permission from Singh et al. (2010b).

Satalkar et al. (2016) in their study of effect of 80 MeV O^{6+} ions on manganese-zinc ferrite nanoparticles also observed the rearrangement of cations at tetrahedral and octahedral sites (Satalkar et al., 2018). Similar results were reported by Raghuvanshi et al. (2019) and Dhyani et al. (2020). Thus, from several studies, it can be inferred that cation redistribution can take place on irradiation. Zinc ferrite nanoparticles annealed at 300, 500, 800, and 1000°C were subjected to irradiation with 200 MeV Ag^{15+} ions and studied by Singh et al. (2012b) XRD analysis showed that the presence of impurity peaks after irradiation for samples annealed at 300 and 500°C. However, nanoparticles annealed 800 and 1000°C were in pure cubic spinel phase even after irradiation. Increased crystallite size was observed for all samples upto a certain fluence due to increase in local temperature as suggested by Kaoumi et al. (2008). At higher fluence crystallite sizes decreased due to the splitting of crystallites. The properties of zinc ferrite thin films formed via RF sputtering technique and irradiated with 100 MeV Ag ions were studied by Raghavan et al. (2017). Decrease in crystallite size was observed on irradiating the pristine samples. It was attributed to the amorphisation of the irradiated material which was explained on the basis of the thermal spike model. When the pristine thin films were irradiated, high-temperature localized zones can melt the material which on rapid cooling led to partial amorphisation of the material. On further irradiating the material with higher fluence, an increase in crystallite size was observed which was attributed to the breaking of crystallites and joining again to form larger crystallites. Nongjai et al. (2015). observed decrease in the intensity of peaks corresponding to planes in the XRD pattern with increase in irradiation fluence on cobalt ferrite thin films. It was also attributed to the partial amorphisation of the material. Progressive amorphisation with increasing fluence in the material was also observed by Dixit et al. (2011) in their study of nickel ferrite thin films irradiated with 200 MeV Ag^{15+} ions. Figure 10 shows that crystalline Nickel ferrite thin films become amorphous after irradiation (Dixit et al., 2011). Balaji et al. (2011) in their study of 150 MeV Ni^{11+} ions irradiated tetragonal phase $CuFe_2O_4$ thin films observed complete amorphisation at higher fluences.

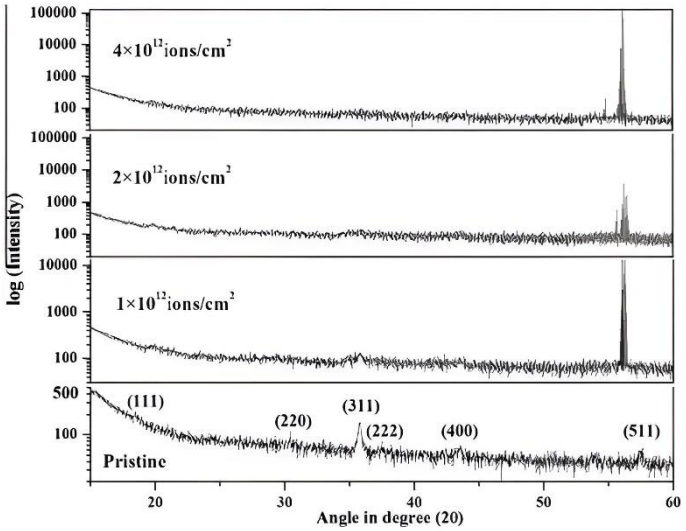

Figure 10. XRD patterns of the pristine and irradiated films of thickness 150 nm at fluences of 1×10^{12}, 2×10^{12} and 4×10^{12} ions/cm^2 of 200 MeV Ag^{15+} ions. Reprinted with permission from Dixit et al. (2011).

Thus, it can be inferred on irradiating the spinel ferrite nanoparticles and thin films with swift heavy ions, deterioration of the crystalline structure, cation redistribution among lattice sites and amorphisation of the material takes place. This leads to a change in crystallite size after irradiation depending on the crystallite size of pristine ferrite as can be seen from Figure 11 (Singh et al., 2011; Singh et al., 2012b).

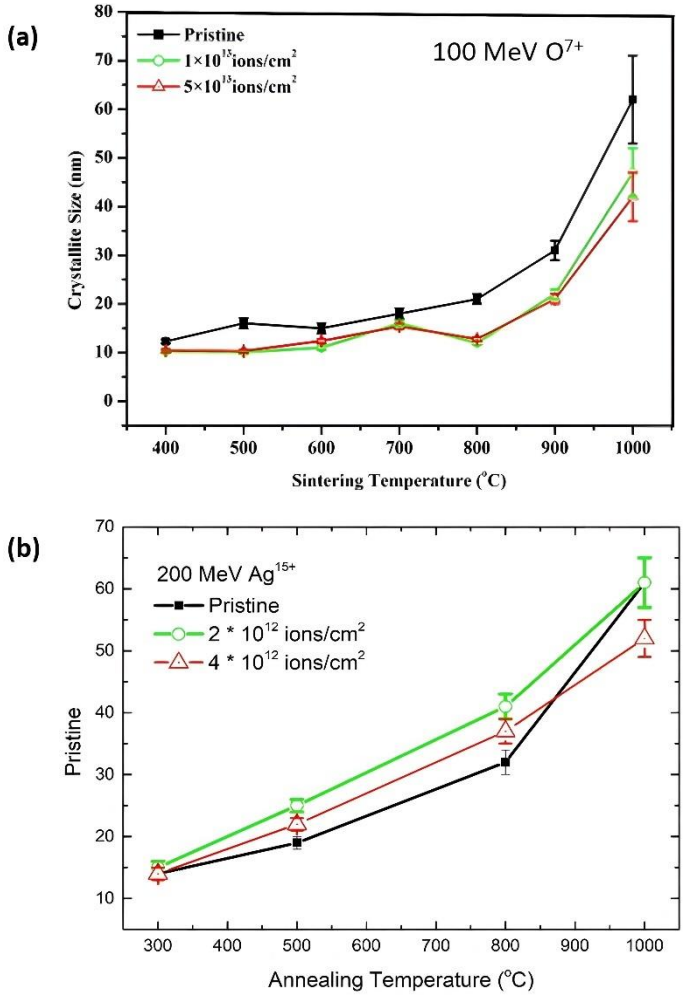

Figure 11. Crystallite size of zinc ferrite nanoparticles under different fluences of (a) 100 MeV O^{7+} reprinted with permission from Singh et al. (2011), and (b) 200 MeV Ag^{15+}. reprinted with permission from Singh et al. (2012b).

4.2 Magnetic Properties

Heavy ion irradiation is known to modify the magnetic behavior of various systems (Kato et al., 2005). Hence, this tool is widely applied to ferrite nanoparticles and modification is associated with either point or columnar defects. The dissipation of energy in the materials during ion beam irradiation is responsible for the formation of latent tracks. It induces the rearrangement in the distribution of cations, the oxygen as well as inversion parameters and produces significant changes in magnetic properties of a typical ferrite (Nongjai et al., 2015). The rearrangement of cations in ferrites depends on the type of selected ions as well as on the energy and fluence range of the ions. The variation in the magnetic parameters (M_S, H_C) of irradiated ferrites in comparison to pristine samples are shown in Table 2.

Ion beam irradiation leads the formation of a non-magnetic layer (also known as dead layer) depending on the ion beams. The non-magnetic layer plays a significant role in the variation of magnetic parameters of ferrites upon SHI irradiation (Raghuvanshi et al., 2019). The canting of the surface spin, high surface anisotropy and heavy ion irradiation are the general causes which leads the formation non-magnetic layers on the ferrites surface (Maehara et al., 2005; Li et al., 2010). Irradiation leads to the formation of a dead

layer on the surface, thus affecting magnetic properties, via spin canting at the surface. The increased thickness of dead layer is ascribed to the effect of spin disorder at the surface of the particle due to irradiation. The thickness (t) of dead layer can be evaluated using the following expression (El-Sayed et al., 2017):

$$t = \frac{D}{6}\left(1 - \frac{M_S}{M_B}\right) \quad (1)$$

where, D, M_s and M_B is grain size, saturation magnetization, bulk magnetization of the ferrite sample, respectively.

The mathematical expression (1) suggests the inverse relationship between M_S and t, which is due to the effect of surface spin disorder upon SHI irradiation. The decrease in the value of M_s can be attributed to the low concentration of Fe^{3+} ions on the B site or the reduction in the inversion parameter upon SHI irradiation (Parmar et al., 2022b). The reduction in oxygen position parameter (u), which is a measure of disorder leads to diminishing strain, hence reducing the coercivity of the sample due to irradiation. Further, It can be verified with the corresponding changes in the cation distribution.

The SHI-irradiated ferrite sample is composed of two regions: one with spins that are aligned with the latent track and another with spins that are randomly distributed. In addition, irradiation may result in a cation inversion, which raises the temperature of the materials exposed to radiation. As a result, the production of directed spin zones in the direction of latent tracks and induced cation inversion is observed.

Also enhanced magnetization and the development of hysteresis were observed after irradiation (Balaji et al., 2011, Raghavan et al., 2017). The physical and chemical characteristics of the irradiated ferrites also vary as a result of extended defective patches and changed cation inversion.

At low fluence, as the accumulation of defects in the ferrite sample induced by SHI irradiation, results in an increase in H_c while the reduction in M_s. It is mainly because of the significant increase in the number of grain boundaries which act as pinning sites of the magnetic domain. Si^{9+} ion-irradiation results in a decrease in oxygen positional parameter, strain, and saturation magnetization as well as an increase in inversion degree, and a reduction in dead-layer thickness. The modification in the A-O-B, A-O-A, and B-O-B super-exchange interaction is also observed upon Si irradiation. The analyzed samples fall in an overlap region between many domains or inside a single domain, according to the linear dependency of coercivity on grain diameter (Parmar et al., 2022b). At high fluence, the electron-phonon coupling is responsible for the change in crystal orientation and the dissociation. After irradiation, the temperature of the sample's surface is enhanced due to the very high energy of incident ion beams (Singh et al., 2022). The thermal spike model suggests that the time required to transfer the energy from an incident ion to an excited electron is far less than the normal time scales of lattice vibrations. The electrons instantly receive the energy from the incident ion and transfer to the excited states (Ghosh et al., 2006) which leads to a momentary increase in temperature of the confined zone along the path of the ion and heat is transmitted to the lattice in the form of energy via electron-phonon coupling. The enhanced local temperature results in the variation in the crystallinity of the sample and alterations in various structural properties.

The nature of strain-induced defects, production mechanisms, atomic motion, relaxation, thermal spike, coulomb explosion, surface morphology, the electronic-excitation effects, etc. is used to interpret changes in magnetic properties after irradiation (Kumar et al., 2009; Singh et al., 2010a; Sun et al., 2012). The structural analysis, surface morphology, and magnetic characteristics of ferrite nanoparticles showed a significant variation upon irradiation, which was supported by a number of ion irradiation experiments. A few of them are summarized in Table 3.

Table 3. Magnetic characteristic of SHI irradiated ferrite materials.

Ferrite	Magnetic Parameters			SHI		Ref.
	D (nm)	**M_s (emu/g)**	**H_c (Oe)**	**Ion**	**Fluence (ions/cm^2)**	
$ZnFe_2O_4$	16	7.8	~	100 MeV O	0	Singh et al. (2010a)
	10.3 ± 0.3	6.6			1×10^{13}	
	12± 0.2	~	18	90KeV, Ne	0	Gafton et al. (2016)
	13± 0.8	~	74		$3x10^{14}$	
	17.4	0 μB	~	80 MeV, O	0	Satalkar et al. (2018)
	15.7	8.5 μB	~		$1x10^{11}$	
$NiFe_2O_4$	42.82	33.02	157	120 MeV, Si	0	Sharma et al. (2018)
	36.33	20.32	163		$1x10^{12}$	
$Ni_{0.5}Zn_{0.5}Fe_2O_4$	33.10	49.68	85.45	120 MeV, Si	$1x10^{12}$	Sharma et al. (2018)
	32.51	18.60	89.0			
$Ni_{0.65}Zn_{0.375}In_{0.25}Ti_{0.025}Fe_{1.70}O_4$	6.8	~	~	190 MeV Ag	0	Rao et al. (2006)
	5.2	~	~		$1x10^{13}$	
$MnFe_2O_4$	10.04	5	~	80 MeV, O	0	Satalkar et al. (2016)
	9.98	~	~		$1x10^{13}$	
$Mn_{0.75}Zn_{0.18}Fe_{2.07}O_4$	3.9	~	~	190 MeV, Ag	0	Rao et al. (2006)
	2.4	~	~		$1x10^{13}$	
$MgFe_2O_4$	34.7	23.8	106	120 MeV, Si	0	Raghuvanshi et al. (2019)
	31.0	15.6	103		1×10^{11}	
$CuFe_2O_4$	10	5.50	22.698	150 MeV, Ni	0	Balaji et al. (2011)
	~	4.195	54.875		5×10^{14}	

4.3 Optical Behavior

Though the optical behaviour of ferrite is an important characteristic but it is rarely reported for irradiated nanoparticle systems. To investigate the effect on the optical properties of irradiated zinc ferrite system, optical measurements were performed on the zinc ferrite nanoparticles having crystallite sizes of 10 (ZF300), 16 (ZF500), 21 (ZF800) and 62 nm (ZF1000). UV-VIS absorption spectra of the pristine (P) and irradiated (I) samples recorded at room temperature are shown in Figure 12. All the spectra exhibit strong absorption in the UV-region which is characteristic of ferrites (Muret, 1974). This effect is observed for both pristine and irradiated counterpart

The absorption coefficient, α, for both the pristine and irradiated samples was determined by using the relation (Fox, 2001; Joshi et al., 2003).

$$\alpha = 2.303\frac{Absorbance}{t}.$$

t is the thickness of the cuvette (*t*=1cm).

Figure 13 shows α versus hν plot for the pristine and irradiated samples. We have estimated the optical band gap of samples by using the Tauc's relation (Tauc, 2012). The optical gap from this relation was estimated by plotting $(\alpha h\nu)1/m$ versus hν and by extrapolating a straight line for m= ½ (as elaborated by Singh et al., 2010b). The value of the optical band-gap varies from 3.8 eV to 3.65 eV with respect to the sintering temperature for the pristine samples. The detailed investigation related to this effect has been attributed to the quantum confinement and discussed elsewhere (Singh et al., 2010b). The values of optical band-gap were found to increase to a value of ~4.37 eV in the case of irradiated samples as compared to the pristine sample. The values of optical band-gap remain constant for irradiated materials at all sintering temperatures. The values of the band-gap for irradiated ferrites are of the order of 4.4 eV. This suggests a dominant contribution from intra–d and d-s transition to the UV-VIS spectra (Schmitt et al., 1987).

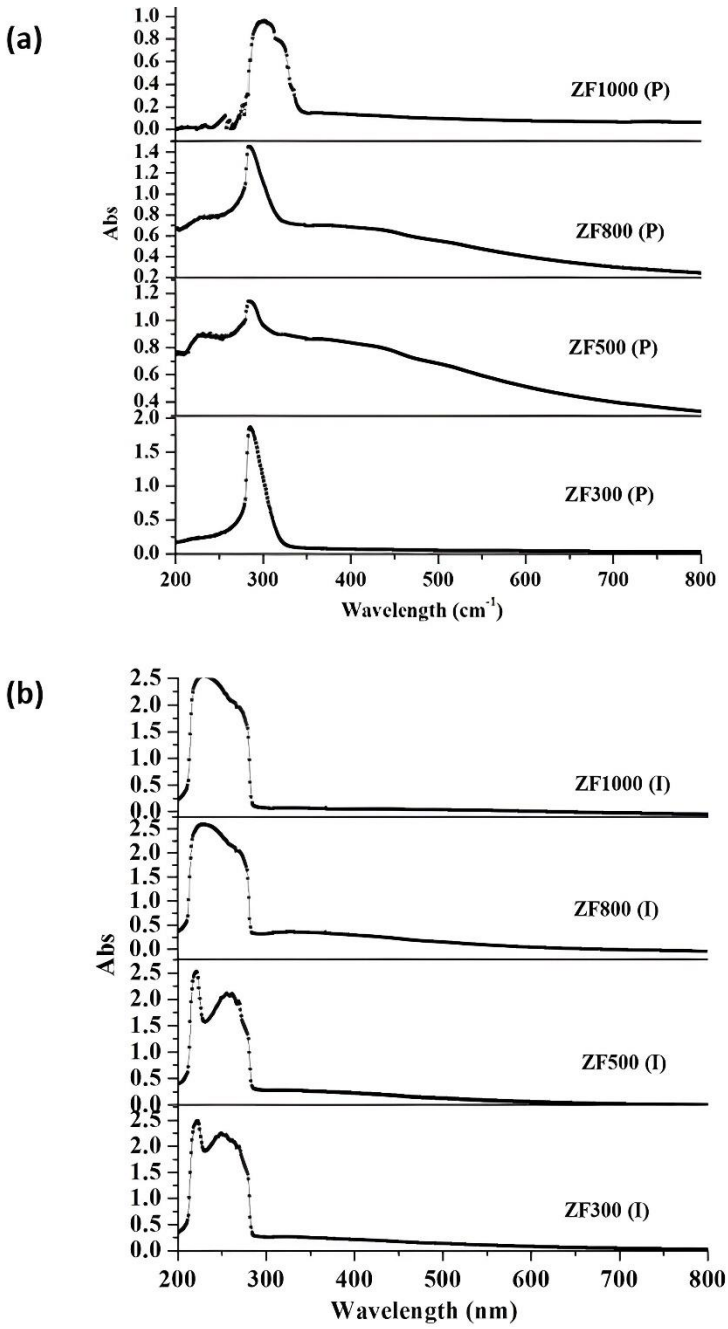

Figure 12. UV-Vis absorption spectra of the (a) pristine (P) Reprinted with permission from Singh et al. (2010b), and (b) irradiated (I) counterpart at room temperature for $ZnFe_2O_4$ nanoparticles under 100 MeV O^{7+} ions.

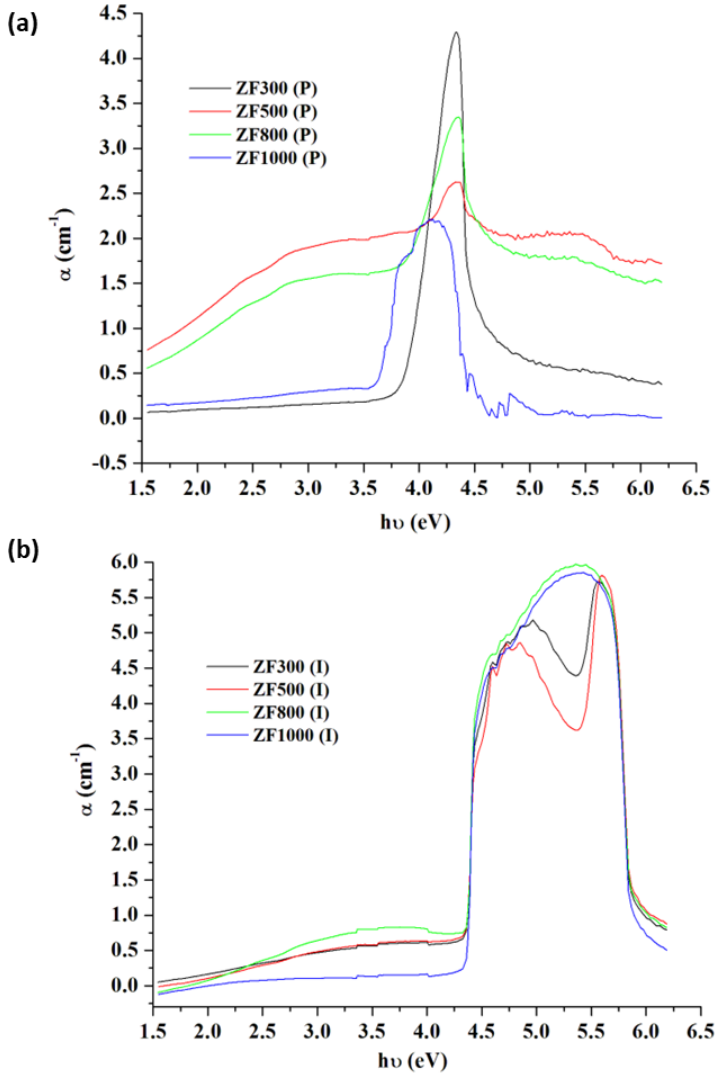

Figure 13. (a) α versus hν for the (a) pristine (P), and (b) irradiated (I) samples.

The particle size of irradiated ferrites is small as compared to that of pristine as shown in Figure 11(a), therefore optical band-gap increases after irradiation. Besides this, the presence of point defects induced by irradiation in ferrites may cause an effective mass of carriers to decrease, resulting in enhancement in the band-gap of these ferrites (Singh, 2002). Hence, the increase of optical band-gap may be attributed to the cumulative effect of both effects. To elucidate the effect of defects on UV-VIS spectra, the position of maxima and full width at half maximum (FWHM) of the absorption peak were estimated and shown in Table 4. The FWHM of the irradiated samples is very much large (~1.38 eV) as compared to the pristine (~0.33 eV). This large value of FWHM is attributed to the increase in defect density in the case of irradiated samples. Similar behavior of irradiated material was also depicted for In_2O_3 on the basis of photoluminescence spectroscopy (Tripathi & Rath, 2014). The maxima of absorption peaks are of the order of 4.34 eV for the pristine samples and these shifted to a value of ~5.5 eV for the irradiated samples. In the case of irradiated samples, we also observe maxima at 4.95 eV for the sample ZF300 (I) and at 4.76 eV for

ZF500 (I). This shows the formation of sub-levels in the small-sized irradiated samples, thereby affecting the optical behaviour of irradiated nanoferrites.

Table 4. Maxima, FWHM of UV-VIS absorption peak for the pristine (P) and irradiated (I) zinc ferrite at different sintering temperatures.

Sintering Temperature (°C)	Crystallite size (nm)	Maxima (eV)		FWHM (eV)	
		P	I	P	I
300	10	4.34	4.95, 5.56	0.34	1.39
500	16	4.34	4.76,5.60	0.25	1.40
800	21	4.34	5.36	0.33	1.39
1000	62	3.75	5.36	0.60	1.38

Apart from the changes in structural, magnetic and optical properties, few reports are available showing the modification in dielectric behavior of ferrites under heavy ion irradiation (Dolia et al., 2012, Dolia et al., 2013). Fe_3O_4 thin films are investigated to observe modification in electrical behavior under 190 MeV Ag^{15+} ions (Kumar et al., 2006). Both the electrical and dielectric behavior are subjected to changes in microstructure, cation redistribution. Thus, almost reports studying the irradiation induced effects strongly emphasize the role of cation redistribution as well as the change in the size of nanoparticles under heavy ion irradiation. This behavior of ferrites corroborates the behavior of native ferrite. However, research work from our group confirms the possibility of cation redistribution without changing crystallite size. These are discussed in next section.

5. Heavy Ion Irradiation Towards Control of Cation Inversion without Changing Size

Thus, these studies clearly depict variation of various properties with heavy ion irradiation and depict the usefulness of heavy ion irradiation. These studies show that size dependent behavior of ferrites is critical even though they are subjected to external effects. However, irradiation carried out on the zinc ferrite nanoparticles shows the reduction of cation inversion factor from 0.56 to 0.24 as estimated from in-field Mössbauer spectroscopy after irradiation from 100 MeV O^{7+} ions. In this case, crystallite size remains to be same (~10 nm) after irradiation (Singh et al., 2010b). Similar behavior is reported for zinc ferrite nanoparticles of almost 12 nm using X-ray absorption fine structure measurements (EXAFS) and X-ray diffraction measurements (Singh et al., 2018). Fe *K*-EXAFS measurements reveal decrease of cation inversion from 0.39 to 0.24 (Figure 14).

In another work from our group, we observed that the crystallite size of $CoFe_2O_4$ remains almost the same within experimental error under the different fluence of 100 MeV O^{7+} ions (Figure 15).

Mössbauer spectroscopy studies carried out on these sample shows changes in cation occupancy which results modification in cation inversion parameters (Kumar et al., 2015b). Thus, these studies may provide an opportunity to researchers to think of heavy ion irradiation with ferrite in different ways. It can provide a scope to manipulate ferrite characteristics without altering crystallite/particle size. Thus, heavy ions can persist a new way to design ferrite for different applications.

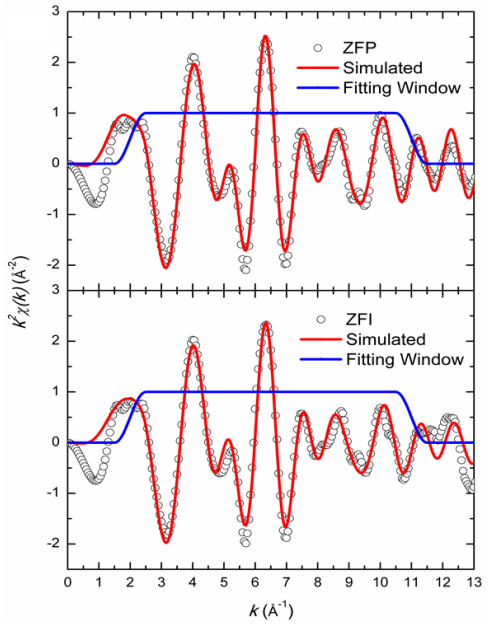

Figure 14. Simulated Fe K-edge EXAFS spectra of pristine (ZFP) and irradiated (ZFI) zinc ferrite. Reprinted with permission from Singh et al. (2018).

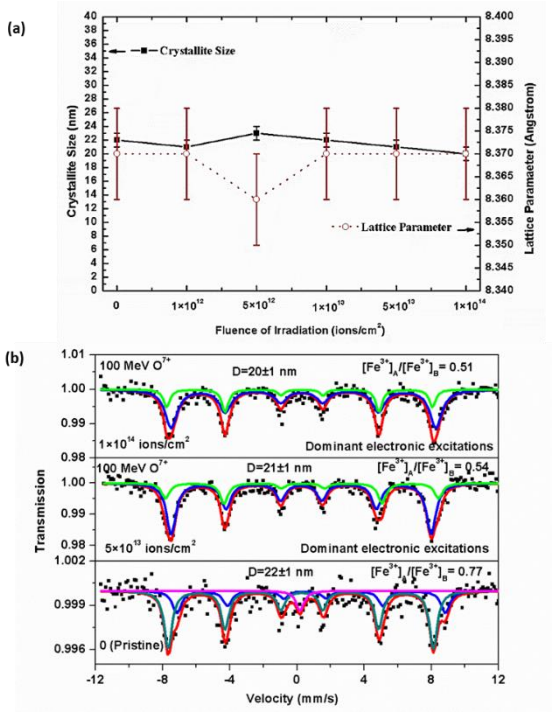

Figure 15. (a) Crystallite size and lattice parameter as a function of the fluence of irradiation (b) Mössbauer spectra of pristine and irradiated ferrite sample showing cation redistribution. Permission is required from Kumar et al. (2015b).

6. Conclusion

Thus, we have provided a critical and in-depth review of irradiation studies in ferrites. Ferrite which is well known to exhibit size-dependent behavior shows this behavior even when subjected to external tools such as swift heavy ion irradiation. Recent research also shows that it can be an effective tool to control cation occupancy in ferrites without changing the crystallite size. This can ultimately be used to tailor the physical properties of ferrites by keeping crystallite size as a constant parameter.

Conflict of Interest

The authors confirm that there is no conflict of interest to declare for this publication.

Acknowledgments

This research did not receive any specific grant from funding agencies in the public, commercial, or not-for-profit sectors. The authors would like to thank the editor and anonymous reviewers for their comments that helped improve the quality of this work.

References

Abdelmoneim, H.M. (2010). Optical properties of Ti0. 5Li0. 5La0. 1Fe1. 9O4 ferrite thin film. *Physica B: Condensed Matter*, *405*(6), 1551-1557.

Ai, W., Xu, L., Nan, S., Zhai, P., Li, W., Li, Z., Hu, P., Zeng, J., Zhang, S., Liu, L., Sun, Y., & Liu, J. (2019). Radiation damage in β-Ga2O3 induced by swift heavy ions. *Japanese Journal of Applied Physics*, *58*(12), 120914.

Aithal, P.S. (1997). Effect of heavy ion irradiation on dielectric constant and electrical conductivity of doped and undoped nonlinear substance. *Bulletin of Materials Science*, *20*(5), 1069-1077.

Aslibeiki, B., Kameli, P., & Ehsani, M.H. (2016). MnFe2O4 bulk, nanoparticles and film: A comparative study of structural and magnetic properties. *Ceramics International*, *42*(11), 12789-12795.

Ateia, E.E., Ghaffar, D.N., Badr, Y., & Fangary, N. (2019). Nd: YAG laser irradiation effect on the physical properties of cobalt ferrite nanoparticles. *Applied Physics A*, *125*, 1-8.

Bagwan, A.M., Waikar, M.R., Sonker, R.K., Chakarvarti, S.K., & Sonkawade, R.G. (2022). Gas sensor based on ferrite materials. In Sonker, R.K., Singh, K., Sonkawade, R. (eds) *Smart Nanostructure Materials and Sensor Technology* (pp. 285-307). Springer, Singapore.

Balaji, M., Raja, M.M., Asokan, K., Kanjilal, D., Rajasekaran, T.R., & Padiyan, D.P. (2011). Effect of thermal spike energy created in CuFe2O4 by 150 MeV Ni11+ swift heavy ion irradiation. *Nuclear Instruments and Methods in Physics Research Section B: Beam Interactions with Materials and Atoms*, *269*(10), 1088-1093.

Bharathi, M.N., Pushpa, N., Vinayakprasanna, N.H., & Prakash, A.G. (2016). A comparison of lower and higher LET heavy ion irradiation effects on silicon NPN rf power transistors. *Nuclear Instruments and Methods in Physics Research Section A: Accelerators, Spectrometers, Detectors and Associated Equipment*, *822*, 34-42.

Brockman, F.G. (1951). Structure and properties of ferrites. *Electrical Engineering*, *70*(6), 489-494.

Cannavò, A., Vacik, J., Lavrentiev, V., Ceccio, G., Horak, P., Vasi, S., & Bakardjieva, S. (2021). Effect of 2 MeV W+ ion irradiation on the surface morphology of Sc: In: C and Zr: In: C thin films. *Radiation Effects and Defects in Solids*, *176*(11-12), 1049-1064.

Chandramohan, S., Sathyamoorthy, R., Sudhagar, P., Kanjilal, D., Kabiraj, D., & Asokan, K. (2007). Swift heavy ion beam irradiation induced modifications in structural, morphological and optical properties of CdS thin films. *Nuclear Instruments and Methods in Physics Research Section B: Beam Interactions with Materials and Atoms*, *254*(2), 236-242.

Cilleruelo, C., García, E., Moliner, R., Ibarra, J.V., Pineda, M., Fierro, J.L.G., & Palacios, L.M. (1995). Hot gas desulfurization using zinc-ferrite regenerable sorbents. *Coal Science and Technology 24*, 1883-1886. Elsevier. https://doi.org/10.1016/S0167-9449(06)80186-2.

Das, A., Bestha, K.K., Bongurala, P., & Gorige, V. (2020). Correlation between size, shape and magnetic anisotropy of CoFe2O4 ferrite nanoparticles. *Nanotechnology*, *31*(33), 335716.

Dhyani, R., Joshi, L., Rawat, P.S., Dixit, G., Srivastava, R.C., & Asokan, K. (2020). Structural and optical study of oxygen irradiated rare earth doped nickel ferrite. In *Journal of Physics: Conference Series* (Vol. 1504, No. 1, p. 012016). IOP Publishing. Jaipur, India.

Dixit, G., Singh, J.P., Srivastava, R.C., & Agrawal, H.M. (2011). Study of 200 MeV Ag15+ ion induced amorphisation in nickel ferrite thin films. *Nuclear Instruments and Methods in Physics Research Section B: Beam Interactions with Materials and Atoms*, *269*(2), 133-139.

Dixit, G., Singh, J.P., Srivastava, R.C., & Agrawal, H.M. (2012b). Magnetic resonance study of Ce and Gd doped NiFe2O4 nanoparticles. *Journal of Magnetism and Magnetic Materials*, *324*(4), 479-483.

Dixit, G., Singh, J.P., Srivastava, R.C., Agrawal, H.M., & Asokan, K. (2012c). Swift heavy ion-induced effects in Ce-doped nickel ferrite nanoparticles. *Radiation Effects and Defects in Solids*, *167*(5), 307-318.

Dixit, G., Singh, J.P., Srivastava, R.C., Agrawal, H.M., & Chaudhary, R.J. (2012a). Structural, magnetic and optical studies of nickel ferrite thin films. *Advanced Materials Letters*, *3*(1), 21-28.

Dolia, S.N., Sharma, P.K., Dhawan, M.S., Kumar, S., Prasad, A.S., Samariya, A., & Saitovitach, E. (2012). Swift heavy ion irradiation induced modifications in magnetic and dielectric properties of Mn–Ca ferrite. *Applied Surface Science*, *258*(9), 4207-4211.

Dolia, S.N., Sharma, P.K., Samariya, A., Pareek, S.P., Prasad, A.S., Dhawan, M. S., & Asokan, K. (2013). 200 MeV Ag+ 15 ion irradiation-induced modifications in structural, magnetic and dielectric properties of nanoparticles of Cu0. 2Zn0. 8Fe2O4 ferrite. *Radiation Effects and Defects in Solids*, *168*(7-8), 537-546.

El-Sayed, H.M., Ali, I.A., Azzam, A., & Sattar, A.A. (2017). Influence of the magnetic dead layer thickness of Mg-Zn ferrites nanoparticle on their magnetic properties. *Journal of Magnetism and Magnetic Materials*, *424*, 226-232.

Fantauzzi, M., Secci, F., Angotzi, M.S., Passiu, C., Cannas, C., & Rossi, A. (2019). Nanostructured spinel cobalt ferrites: Fe and Co chemical state, cation distribution and size effects by X-ray photoelectron spectroscopy. *RSC Advances*, *9*(33), 19171-19179.

Fesharaki, M.J., Nabiyouni, G., Aghamohamadi, M., & Ghanbari, D. (2016). Investigation of size dependent Curie temperature and magnetization of bismuth substituted zinc ferrite (ZnBi x Fe 2− x O 4) nanoparticles. *Journal of Materials Science: Materials in Electronics*, *27*, 4699-4704.

Fox, M. (2001). *Optical properties of solids*. Oxford University Press, New York.

Gafton, E.V., Bulai, G., Caltun, O.F., Cervera, S., Macé, S., Trassinelli, M., Steydli, S., & Vernhet, D. (2016). Structural and magnetic properties of zinc ferrite thin films irradiated by 90 keV neon ions. *Applied Surface Science*, *379*, 171-178.

Garg, S., Gautam, S., Singh, J.P., Kaur, M., Gupta, A., Meena, R., Chakraverty, S., Jung, Y.H., & Goyal, N. (2023). Dissolution of Mg (OH) 2 by swift heavy ion irradiation in CoFe2O4/MgO/ZnFe2O4 multilayer thin films. *Materials Letters*, 134738.

Ghosh, S., Khan, S.A., Ganesan, V., Kundu, S., & Bhattacharya, R. (2006). Surface studies on 100 MeV Ag7+ ions and 150 MeV Ni11+ ions irradiated nanocrystalline ferrite thin films. *Nuclear Instruments and Methods in Physics Research Section B: Beam Interactions with Materials and Atoms*, *244*(1), 34-39.

Grimes, N.W., & Collett, A.J. (1971). Infrared absorption spectra of ferrites. *Nature Physical Science*, *230*(15), 158-158.

Hasirci, C., Karaagac, O., & Köçkar, H. (2019). Superparamagnetic zinc ferrite: a correlation between high magnetizations and nanoparticle sizes as a function of reaction time via hydrothermal process. *Journal of Magnetism and Magnetic Materials*, *474*, 282-286.

Hublikar, L.V., Ganachari, S.V., & Patil, V.B. (2023). Zn and Co ferrite nanoparticles: towards the applications of sensing and adsorption studies. *Environmental Science and Pollution Research*, *30*(25), 66994-67007.

Islam, K., Haque, M., Kumar, A., Hoq, A., Hyder, F., & Hoque, S.M. (2020). Manganese ferrite nanoparticles (MnFe2O4): Size dependence for hyperthermia and negative/positive contrast enhancement in MRI. *Nanomaterials*, *10*(11), 2297.

Jauhar, S., Kaur, J., Goyal, A., & Singhal, S. (2016). Tuning the properties of cobalt ferrite: A road towards diverse applications. *RSC Advances*, *6*(100), 97694-97719.

Jha, M.C., Blandon, A.E., & Hepworth, M.T. (1988). *U.S. Patent No. 4,732,888*. Washington, DC: U.S. Patent and Trademark Office.

Jiang, S., Zhu, R., Chen, M., He, H., Lin, Z., Hu, X., Zhang, J., Cao, L., & Huang, Z. (2021). In-situ He+ irradiation induced crystallization on crystalline/amorphous ZrC films. *Materials Today Communications*, *28*, 102580.

Jogi, J.K., Singhal, S.K., Jangir, R., Dwivedi, A., Tanna, A.R., Singh, R., Gupta, M.,. & Sagdeo, P.R. (2022). Investigation of the structural and optical properties of zinc ferrite nanoparticles synthesized via a green route. *Journal of Electronic Materials*, *51*(10), 5482-5491.

Joshi, G.P., Saxena, N.S., Mangal, R., Mishra, A., & Sharma, T.P. (2003). Band gap determination of Ni-Zn ferrites. *Bulletin of Materials Science*, *26*, 387-389.

Kamble, R.B., Varade, V., Ramesh, K.P., & Prasad, V. (2015). Domain size correlated magnetic properties and electrical impedance of size dependent nickel ferrite nanoparticles. *AIP Advances*, *5*, 017119.

Kaoumi, D., Motta, A.T., & Birtcher, R.C. (2008). A thermal spike model of grain growth under irradiation. *Journal of Applied Physics*, *104*, 073525. https://doi.org/10.1063/1.2988142.

Karmakar, S., & Behera, D. (2020). Magnetic and optical studies of NiFe 2 O 4 micro-and nanoparticles. *Journal of Superconductivity and Novel Magnetism*, *33*, 1619-1627.

Kato, H., Hamaya, K., Kitamoto, Y., Taniyama, T., & Munekata, H. (2005). Effect of Ga+ irradiation on magnetic and magnetotransport properties in (Ga, Mn) As epilayers. *Journal of Applied Physics*, *97*(10). 10D302. https://doi.org/10.1063/1.1844751.

Kumar, H., Negi, P., Singh, J.P., Srivastava, R.C., Ambreen, S., & Asokan, K. (2023). Tuning of structural, electrical and transport behaviour of cobalt nanoferrite by dysprosium ions substitution. *Ceramics International*, *49*(16), 27294-27302.

Kumar, H., Singh, J.P., Srivastava, R.C., Negi, P., Agrawal, H.M., Asokan, K., Won, S.O., & Chae, K.H. (2015a). Consequences of electronic excitations in CoFe1. 90Dy0. 10O4. *Current Applied Physics*, *15*(12), 1650-1656.

Kumar, H., Singh, J.P., Srivastava, R.C., Negi, P., Agrawal, H.M., Asokan, K., Won, S.O., & Chae, K.H. (2015b). Onset of size independent cationic exchange in nano-sized CoFe2O4 induced by electronic excitation. *Journal of Alloys and Compounds*, *645*, 274-282.

Kumar, M.K.S., Kumar, E.R., Srinivas, C., Prasad, G., Meena, S.S., Pradeep, I., Suriyanarayanan, N., & Sastry, D.L. (2019). Structural and magnetic properties of CuFe2O4 ferrite nanoparticles synthesized by cow urine assisted combustion method. *Journal of Magnetism and Magnetic Materials*, *484*, 120-125.

Kumar, P., Singh, J.P., Kumar, V., & Asokan, K. (2022). *Ion beam induced defects and their effects in oxide materials*. Springer. Switzerland.

Kumar, R., Khan, M.W., Srivastava, J.P., Arora, S.K., Sofin, R.G.S., Choudhary, R.J., & Shvets, I.V. (2006). Swift heavy ion irradiation-induced modifications in structural, magnetic and electrical transport properties of epitaxial magnetite thin films. *Journal of Applied Physics*, *100*, 033703. https://doi.org/10.1063/1.2222066.

Kumar, R., Sharma, S.K., Dogra, A., Kumar, V.S., Dolia, S.N., Gupta, A., Khonbel, M., & Singh, M. (2005). Magnetic study of nanocrystalline ferrites and the effect of swift heavy ion irradiation. In *IWNMS 2004: Proceedings of the International Workshop on Nanomaterials, Magnetic Ions and Magnetic Semiconductors Studied Mostly by Hyperfine Interactions* (pp. 143-156), Baroda, India.

Kumar, S., Sharma, S.K., Choudhary, R.J., Lee, C.G., Koo, B.H., & Kumar, R. (2009). Engineering structural and magnetic properties of Mg0. 95Mn0. 05Fe2O4 thin films using 200 MeV Au ions. *Journal of the Ceramic Society of Japan*, *117*(1365), 685-688.

Kumar, V., Kumar, S., Maan, A.S., & Akhtar, J. (2023). Interfacial and structural analysis of MeV heavy ion irradiated SiC. *Applied Nanoscience*, *13*(5), 3181-3188.

Kuzmann, E., Nomura, K., Stichleutner, S., Nakanishi, A., Pechousek, J., Machala, L., Homonnay, Z., Vondrasek, R., Skuratov, V.A., Krupa, L., Malina, O., Ingr, T., & Kubuki, S. (2023). Swift heavy ion irradiation-induced amorphous iron and Fe–Si oxide phases in metallic 57 Fe layer vacuum deposited on surface of SiO 2/Si. *Journal of Materials Research*, *38*(4), 1061-1073.

Lahouli, R., Massoudi, J., Smari, M., Rahmouni, H., Khirouni, K., Dhahri, E., & Bessais, L. (2019). Investigation of annealing effects on the physical properties of $Ni_{0.6}Zn_{0.4}Fe_{1.5}Al_{0.5}O_4$ ferrite. *RSC Advances*, *9*(35), 19949-19964.

Lamouri, R., Fkhar, L., Salmani, E., Mounkachi, O., Hamedoun, M., Ali, M.A., Benyoussef, A., & Ez-Zahraouy, H. (2020). A combined experimental and theoretical study of the magnetic properties of bulk $CoFe_2O_4$. *Applied Physics A*, *126*, 1-6.

Lamouri, R., Mounkachi, O., Salmani, E., Hamedoun, M., Benyoussef, A., & Ez-Zahraouy, H. (2020b). Size effect on the magnetic properties of CoFe2O4 nanoparticles: a Monte Carlo study. *Ceramics International*, *46*(6), 8092-8096.

Li, G., Zhu, X., Song, W., Yang, Z., Dai, J., Sun, Y., & Fu, Y. (2011). Annealing effects on semitransparent and ferromagnetic ZnFe2O4 nanostructured films by Sol–Gel. *Journal of the American Ceramic Society*, *94*(9), 2872-2877.

Li, J., Meng, Q., Zhang, Y., Peng, L., Yu, G., Marschilok, A.C., Wu, L., Su, D., Takeuchi, K.J., Takeuchi, E.S., Zhu, Y., & Stach, E.A. (2019). Size-dependent kinetics during non-equilibrium lithiation of nano-sized zinc ferrite. *Nature Communications*, *10*(1), 93. https://doi.org/10.1038/s41467-018-07831-5.

Li, Z., Kawashita, M., Araki, N., Mitsumori, M., Hiraoka, M., & Doi, M. (2010). Magnetite nanoparticles with high heating efficiencies for application in the hyperthermia of cancer. *Materials Science and Engineering: C*, *30*(7), 990-996.

Liu, C., & Zhang, Z.J. (2001). Size-dependent superparamagnetic properties of Mn spinel ferrite nanoparticles synthesized from reverse micelles. *Chemistry of Materials*, *13*(6), 2092-2096.

Lord, H., & Parker, R. (1960). Electrical resistivity of nickel ferrite. *Nature*, *188*(4754), 929-930.

Lu, R.E., Chang, K.G., Fu, B., Shen, Y.J., Xu, M.W., Yang, S., & Yang, Y. D. (2014). Magnetic properties of different CoFe 2 O 4 nanostructures: nanofibers versus nanoparticles. *Journal of Materials Chemistry C*, *2*, 8578-8584.

Maehara, T., Konishi, K., Kamimori, T., Aono, H., Hirazawa, H., Naohara, T., & Kawachi, K. (2005). Selection of ferrite powder for thermal coagulation therapy with alternating magnetic field. *Journal of Materials Science*, *40*, 135-138.

Massoudi, J., Smari, M., Nouri, K., Dhahri, E., Khirouni, K., Bertaina, S., & Bessais, L. (2020). Magnetic and spectroscopic properties of Ni–Zn–Al ferrite spinel: From the nanoscale to microscale. *RSC Advances*, *10*(57), 34556-34580.

Mohapatra, J., Xing, M., & Liu, J.P. (2019). Inductive thermal effect of ferrite magnetic nanoparticles. *Materials*, *12*(19), 3208.

Mozaffari, M., & Masoudi, H. (2014). Zinc ferrite nanoparticles: new preparation method and magnetic properties. *Journal of Superconductivity and Novel Magnetism*, *27*, 2563-2567.

Muret, P. (1974). Optical absorption in polycrystalline thin films of magnetite at room temperature. *Solid State Communications*, *14*(11), 1119-1122.

Nandy, S., Latwal, M., Pandey, G., & Chae, K.H. (2022). Synthesis of Nanostructured Ferrites and Cation Distribution Studies by X-ray Magnetic Circular Dichroism, Mössbauer Spectroscopy, and X-ray Absorption Spectroscopy. *Journal of Electronic Materials*, *51*(12), 6663-6688.

Narang, S.B., & Pubby, K. (2021). Nickel spinel ferrites: A review. *Journal of Magnetism and Magnetic Materials*, *519*, 167163.

Nongjai, R., Chae, K.H., Srivastava, R.C., & Kandasami, A. (2023). Swift heavy ion irradiation effects in ferrite nanostructures. In *Ferrite Nanostructured Magnetic Materials* (pp. 407-430). Woodhead Publishing.

Nongjai, R., Khan, S., Ahmed, H., Khan, I., Annapoorni, S., Gautam, S., Gautam, S., & Asokan, K. (2015). Modification of magnetic anisotropy induced by swift heavy ion irradiation in cobalt ferrite thin films. *Journal of Magnetism and Magnetic Materials*, *394*, 432-438.

Noreen, Z., Ahmad, I., Siddiqui, F., Ziya, A.B., Abbas, T., & Bokhari, H. (2017). Size dependent structural, anti-bacterial and anti-biofilm properties of Er doped Li-Ni ferrites synthesized by the sol-gel auto-combustion route. *Ceramics International*, *43*(14), 10784-10790.

Panda, R., Khan, S.A., Singh, U.P., Naik, R., & Mishra, N.C. (2021). The impact of fluence dependent 120 MeV Ag swift heavy ion irradiation on the changes in structural, electronic, and optical properties of AgInSe 2 nano-crystalline thin films for optoelectronic applications. *RSC Advances*, *11*(42), 26218-26227.

Pang, L., Cui, M., Shen, T., Gao, X., Wei, K., Tai, P., Yao C., Chang, H., Jin, P., & Wang, Z. (2021). Effect of heavy ions irradiation on LiTaO3 crystal. *Results in Physics*, *22*, 103861.

Parmar, C., Verma, R., Modak, S.S., Mazaleyrat, F., & Kane, S.N. (2022b). Si9+ Ion-irradiation induced modification of structural and magnetic properties of Zn-nanoferrite. *ECS Journal of Solid State Science and Technology*, *11*(5), 053015.

Parmar, K.P.S., Kim, J.H., Bist, A., Dua, P., Tiwari, P.K., Phuruangrat, A., & Lee, J.S. (2022a). Superparamagnetic and perfect-paramagnetic zinc ferrite quantum dots from microwave-assisted tunable synthesis. *ACS omega*, *7*(35), 31607-31611.

Pascard, H., & Studer, F. (1997). Review of irradiation effects on ferrites: Results in the world from 1970 to 1995. *Le Journal de Physique IV*, *7*(C1), C1-211.

Peddis, D., Orrù, F., Ardu, A., Cannas, C., Musinu, A., & Piccaluga, G. (2012). Interparticle interactions and magnetic anisotropy in cobalt ferrite nanoparticles: Influence of molecular coating. *Chemistry of Materials*, *24*(6), 1062-1071.

Peng, E., Wei, X., Herng, T.S., Garbe, U., Yu, D., & Ding, J. (2017). Ferrite-based soft and hard magnetic structures by extrusion free-forming. *RSC Advances*, *7*(43), 27128-27138.

Péter, J. (1977). Deep inelastic collisions with heavy ions: Experiments. *Nuclear Instruments and Methods*, *146*(1), 225-234.

Pham, T.N., Trang, N.L.N., Dinh, N.X., Hoa, N.Q., Tuan, D.A., & Le, A.T. (2023). Exploiting the effect of inversion degree, phase, and size in nickel ferrite nanoparticles: implications for electrochemical behaviors and magnetic hyperthermia properties. *Sensors and Actuators A: Physical*, 359, 114511.

Raghavan, L., Joy, P.A., Vijaykumar, B.V., Ramanujan, R.V., & Anantharaman, M.R. (2017). Defect induced modification of structural, topographical and magnetic properties of zinc ferrite thin films by swift heavy ion irradiation. *Nuclear Instruments and Methods in Physics Research Section B: Beam Interactions with Materials and Atoms*, *396*, 68-74.

Raghavan, L., Pookat, G., Thomas, H., Ojha, S., Avasthi, D.K., & Anantharaman, M.R. (2015). Room temperature ferrimagnetism and low temperature disorder effects in zinc ferrite thin films. *Journal of Magnetism and Magnetic Materials*, *385*, 265-271.

Raghuvanshi, S., Tiwari, P., Kane, S.N., Avasthi, D.K., Mazaleyrat, F., Tatarchuk, T., & Mironyuk, I. (2019). Dual control on structure and magnetic properties of Mg ferrite: Role of swift heavy ion irradiation. *Journal of Magnetism and Magnetic Materials*, *471*, 521-528.

Ramola, R.C., Negi, S., Singh, R.C., & Singh, F. (2022). Gas sensing response of ion beam irradiated Ga-doped ZnO thin films. *Scientific Reports*, *12*(1), 22351. https://doi.org/10.1038/s41598-022-26948-8.

Rao, B.P., Rao, K.H., Rao, P.S., Kumar, A.M., Murthy, Y.L.N., Asokan, K., & Caltun, O.F. (2006). Swift heavy ions irradiation studies on some ferrite nanoparticles. *Nuclear Instruments and Methods in Physics Research Section B: Beam Interactions with Materials and Atoms*, *244*(1), 27-30.

Raut, S.D., Awasarmol, V.V., Ghule, B.G., Shaikh, S.F., Gore, S.K., Sharma, R.P., & Mane, R.S. (2018). γ-irradiation induced zinc ferrites and their enhanced room-temperature ammonia gas sensing properties. *Materials Research Express*, *5*(3), 035702.

Refat, N.M., Nassar, M.Y., & Sadeek, S.A. (2022). A controllable one-pot hydrothermal synthesis of spherical cobalt ferrite nanoparticles: Synthesis, characterization, and optical properties. *RSC Advances*,*12*(38), 25081-25095.

Sadeh, B., Doi, M., Shimizu, T., & Matsui, M. (2000). Dependence of the curie temperature on the diameter of fe~ 3o~ 4 ultra-fine particles. *Journal-Magnetics Society of Japan*, *24*(4/2), 511-514.

Satalkar, M., Kane, S.N., & Raghuvanshi, S. (2018). On the O^{6+} ion irradiation induced magnetic moment generation in $ZnFe_2O_4$ nano ferrite. *AIP Conference Proceedings* 1953(1), 030069.

Satalkar, M., Kane, S.N., Kulriya, P.K., & Avasthi, D.K. (2016). Swift heavy ion irradiated spinel ferrite: A cheap radiation resistant material. *Nuclear Instruments and Methods in Physics Research Section B: Beam Interactions with Materials and Atoms*, *379*, 235-241.

Sathyavathi, P., Chavan, S.T., Kanjilal, D., & Bhoraskar, V.N. (1999). Heavy ion induced damage in crystalline silicon and diodes. *Nuclear Instruments and Methods in Physics Research Section B: Beam Interactions with Materials and Atoms*, *156*(1-4), 72-77.

Sato, T., Iijima, T., Seki, M., & Inagaki, N. (1987). Magnetic properties of ultrafine ferrite particles. *Journal of Magnetism and Magnetic Materials*, *65*(2-3), 252-256.

Schmitt-Rink, S.D.A.B.M., Miller, D.A.B., & Chemla, D.S. (1987). Theory of the linear and nonlinear optical properties of semiconductor microcrystallites. *Physical Review B*, *35*(15), 8113-8125.

Šepelák, V., Bergmann, I., Menzel, D., Feldhoff, A., Heitjans, P., Litterst, F.J., & Becker, K.D. (2007). Magnetization enhancement in nanosized MgFe2O4 prepared by mechanosynthesis. *Journal of Magnetism and Magnetic Materials*, *316*(2), e764-e767.

Sharma, A., Devi, K.D., Lim, W.C., & Chae, K.H. (2023a). Ion implantation in ferrites. In *Ferrite Nanostructured Magnetic Materials* (pp. 431-451). Woodhead Publishing.

Sharma, R., Raghuvanshi, S., Satalkar, M., Kane, S.N., Tatarchuk, T.R., & Mazaleyrat, F. (2018). Effect of 120 MeV 28Si9+ ion irradiation on structural and magnetic properties of NiFe2O4 and Ni0. 5Zn0. 5Fe2O4. In *AIP Conference Proceedings* (Vol. 1953, No. 1). AIP Publishing.

Sharma, V.K., Kumawat, A.K., Rathore, S.S., Sulania, I., Meena, R.C., Kedia, S.K., & Nathawat, D.R. (2023b). The SHI irradiation induced transition to negative dielectric constant phase in K2Bi4Ti4WO18. *Frontiers in Physics*, *11*, 1127118.

Siddique, M.A.N.M.B., & Butt, N.M. (2010). Effect of particle size on degree of inversion in ferrites investigated by Mössbauer spectroscopy. *Physica B: Condensed Matter*, *405*(19), 4211-4215.

Singh, A.K., Srivastava, O.N., & Singh, K. (2017). Shape and size-dependent magnetic properties of Fe 3 O 4 nanoparticles synthesized using piperidine. *Nanoscale Research Letters*, *12*, 1-7.

Singh, J. (2002). Effective mass of charge carriers in amorphous semiconductors and its applications. *Journal of Non-Crystalline Solids*, *299*, 444-448.

Singh, J.P., Chae, K.H., Srivastava, R.C., & Caltun, O. F. (2023). *Ferrite nanostructured magnetic materials: technologies and applications*. Woodhead Publishing.

Singh, J.P., Chen, C.L., Dong, C.L., Srivastava, R.C., Agrawal, H.M., Pong, W.F., & Asokan, K. (2013). Effect of intermediate annealing on the structural, electrical and dielectric properties of zinc ferrite: An XANES investigation. *Science of Advanced Materials*, *5*(2), 171-181.

Singh, J.P., Dixit, G., Kumar, H., Srivastava, R.C., Agrawal, H.M., & Kumar, R. (2014). Formation of latent tracks and their effects on the magnetic properties of nanosized zinc ferrite. *Journal of Magnetism And Magnetic Materials*, *352*, 36-44.

Singh, J.P., Dixit, G., Srivastava, R.C., Agrawal, H.M., Reddy, V.R., & Gupta, A. (2012a). Observation of bulk like magnetic ordering below the blocking temperature in nanosized zinc ferrite. *Journal of Magnetism and Magnetic Materials*, *324*(16), 2553-2559.

Singh, J.P., Dixit, G., Srivastava, R.C., Kumar, H., Agrawal, H.M., & Kumar, R. (2012b). Study of size dependent features of swift heavy ion irradiation in nanosized zinc ferrite. *Journal of Magnetism and Magnetic Materials*, *324*(20), 3306-3312.

Singh, J.P., Dixit, G., Srivastava, R.C., Negi, P., Agrawal, H.M., & Kumar, R. (2013). HRTEM and FTIR investigation of nanosized zinc ferrite irradiated with 100 MeV oxygen ions. *Spectrochimica Acta Part A: Molecular and Biomolecular Spectroscopy*, *107*, 326-333.

Singh, J.P., Kaur, B., Sharma, A., Kim, S.H., Gautam, S., Srivastava, R.C., & Chae, K.H. (2018). Mechanistic insights into the interaction between energetic oxygen ions and nanosized ZnFe 2 O 4: XAS-XMCD investigations. *Physical Chemistry Chemical Physics*, *20*(17), 12084-12096.

Singh, J.P., Lim, W.C., Gautam, S., Asokan, K., & Chae, K.H. (2016). Swift heavy ion irradiation induced effects in Fe/MgO/Fe/Co multilayer. *Materials & Design*, *101*, 72-79.

Singh, J.P., Park, J.Y., Singh, V., Kim, S.H., Lim, W.C., Kumar, H., & Chae, K.H. (2020). Correlating the size and cation inversion factor in context of magnetic and optical behavior of CoFe 2 O 4 nanoparticles. *RSC Advances*, *10*(36), 21259-21269.

Singh, J.P., Srivastava, R.C., & Agrawal, H.M. (2010b). Optical behaviour of zinc ferrite nanoparticles. In *AIP Conference Proceedings* (Vol. 1276, No. 1, pp. 137-143). American Institute of Physics. Assam, India.

Singh, J.P., Srivastava, R.C., Agrawal, H.M., & Kumar, R. (2010a). Magnetic behaviour of nanosized zinc ferrite under heavy ion irradiation. *Nuclear Instruments and Methods in Physics Research Section B: Beam Interactions with Materials and Atoms*, *268*(9), 1422-1426.

Singh, J.P., Srivastava, R.C., Agrawal, H.M., Chand, P., & Kumar, R. (2011). Observation of size dependent attributes on the magnetic resonance of irradiated zinc ferrite nanoparticles. *Current Applied Physics*, *11*(3), 532-537.

Singh, J.P., Srivastava, R.C., Agrawal, H.M., Kumar, R., Reddy, V.R., & Gupta, A. (2010c). Magnetic study of nanostructured zinc ferrite irradiated with 100 MeV O-beam. *Journal of Magnetism and Magnetic Materials*, *322*(13), 1701-1705.

Singh, J.P., Srivastava, R.C., Agrawal, H.M., Kushwaha, R.P.S., Chand, P., & Kumar, R. (2008). EPR study of nanostructured zinc ferrite. *International Journal of Nanoscience*, *7*(01), 21-27.

Smit, J., & Wijn, H.P.J. (1954). Physical properties of ferrites. *Advances in Electronics and Electron Physics*, *6*, 69-136.

Srivastava, R.C., Singh, J.P., Agrawal, H.M., Kumar, R., Tripathi, A., Tripathi, R.P., Reddy, V.R., & Gupta, A. (2010, March). 57Fe Mössbauer investigation of nanostructured zinc ferrite irradiated by 100 MeV oxygen beam. In *Journal of Physics: Conference Series* (Vol. 217, No. 1, p. 012109). IOP Publishing. Vienna, Austria.

Studer, F., Houpert, C., Groult, D., Fan, J.Y., Meftah, A., & Toulemonde, M. (1993). Spontaneous magnetization induced in the spinel ZnFe2O4 by heavy ion irradiation in the electronic stopping power regime. *Nuclear Instruments and Methods in Physics Research Section B: Beam Interactions with Materials and Atoms*, *82*(1), 91-102.

Sun, J., Wang, Z., Wang, Y., Zhu, Y., Pang, L., Shen, T., & Li, F. (2012). Structural and magnetic properties studies on swift heavy ion (SHI) irradiated Fe3O4 thin films. *Nuclear Instruments and Methods in Physics Research Section B: Beam Interactions with Materials and Atoms*, *286*, 277-281.

Tauc, J. (2012). *Amorphous and liquid semiconductors*. Springer Science & Business Media. London.

Tawfik, A., Hamada, I.M., & Hemeda, O.M. (2002). Effect of laser irradiation on the structure and electromechanical properties of Co–Zn ferrite. *Journal of Magnetism and Magnetic Materials*, *250*, 77-82. https://doi.org/10.1016/S0304-8853(02)00357-8.

Torruella, P., Ruiz-Caridad, A., Walls, M., Roca, A.G., López-Ortega, A., Blanco-Portals, J., López-Conesa L., Nogués, J., Peiró F., & Estradé, S. (2018). Atomic-scale determination of cation inversion in spinel-based oxide nanoparticles. *Nano Letters*, *18*(9), 5854-5861.

Tripathi, N., & Rath, S. (2013). Effect of thermal annealing and swift heavy ion irradiation on the optical properties of indium oxide thin films. *ECS Journal of Solid State Science and Technology*, *3*(3), 21-25.

Varma, A., Mukasyan, A.S., Rogachev, A.S., & Manukyan, K.V. (2016). Solution combustion synthesis of nanoscale materials. *Chemical Reviews*, *116*(23), 14493-14586.

Varshney, M., Sharma, A., & Verma, K. D. (2023). Crack formation and optical properties in 175 MeV Au13+ ion beam irradiated CeO2 thin films. *Radiation Effects and Defects in Solids*, 1-12.

Vasundhara, K., Achary, S.N., Deshpande, S.K., Babu, P.D., Meena, S.S., & Tyagi, A.K. (2013). Size dependent magnetic and dielectric properties of nano CoFe2O4 prepared by a salt assisted gel-combustion method. *Journal of Applied Physics*, *113*, 194101.

Weber, W.J., Duffy, D.M., Thomé, L., & Zhang, Y. (2015). The role of electronic energy loss in ion beam modification of materials. *Current Opinion in Solid State and Materials Science*, *19*(1), 1-11.

Wu, X., Luo, X., Cheng, H., Yang, R., & Chen, X. (2023). Recent progresses on ion beam irradiation induced structure and performance modulation of two-dimensional materials. *Nanoscale*, *15*(20), 8925-8947.

Yadav, R.S., Kuřitka, I., Vilcakova, J., Havlica, J., Masilko, J., Kalina, L., Tkacz, J., Švec, J., Enev, V., & Hajdúchová, M. (2017). Impact of grain size and structural changes on magnetic, dielectric, electrical, impedance and modulus spectroscopic characteristics of CoFe2O4 nanoparticles synthesized by honey mediated sol-gel combustion method. *Advances in Natural Sciences: Nanoscience and Nanotechnology*, *8*(4), 045002.

Zhao, P.X., Liu, T.Q., Cai, C., Li, D.Q., Ji, Q.G., He, Z., & Liu, J. (2019). Heavy ion irradiation induced hard error in MTJ of the MRAM memory array. Microelectronics Reliability, 100, 113347. https://doi.org/10.1016/j.microrel.2019.06.039.

Zhuravlev, G.I., Golubkov, L.A., & Strakhova, T.A. (1990). Basic types of microstructure of ferrites and means of obtaining them. *Soviet Powder Metallurgy and Metal Ceramics*, *29*(6), 478-482. https://doi.org/10.1016/j.microrel.2019.06.039.

Ziegler, J.F., & Biersack, J.P. (1985). The stopping and range of ions in matter. In *Treatise on Heavy-Ion Science: Volume 6: Astrophysics, Chemistry, and Condensed Matter* (pp. 93-129). Boston, MA: Springer US.

Ziegler, J.F., Ziegler, M.D., & Biersack, J.P. (2010). SRIM–The stopping and range of ions in matter (2010). *Nuclear Instruments and Methods in Physics Research Section B: Beam Interactions with Materials and Atoms*, *268*(11-12), 1818-1823.

Zorai, A., Souici, A., Dragoe, D., Rivière, E., Ouhenia, S., Belloni, J., & Mostafavi, M. (2023). Superparamagnetic cobalt ferrite nanoparticles synthesized by gamma irradiation. *New Journal of Chemistry*, *47*(5), 2626-2634.

Publisher's Note- Ram Arti Publishers remains neutral regarding jurisdictional claims in published maps and institutional affiliations.